Irrigation Science 34 (2): 85-103 (2016)

Solid-set sprinklers irrigation of field boundaries: Experiments and Modeling

Ouazaa, S. [(1)], Burguete, J. [(2)] and Zapata, N. [(3,*)]

[(1)]Dept. Soil and Water. EEAD-CSIC. Avda. Montañana, 1005. 50059 Zaragoza. Spain. sofiane.ouazaa@eead.csic.es

[(2)] Dept. Soil and Water. EEAD-CSIC. Avda. Montañana, 1005. 50059 Zaragoza. Spain. jburguete@eead.csic.es

[(3, *)] Corresponding author. Dept. Soil and Water. EEAD-CSIC. Avda. Montañana, 1005. 50059 Zaragoza. Spain. v.zapata@csic.es

Solid-set sprinklers irrigation of field boundaries: Experiments and Modeling

Abstract:

Numerous studies have analyzed the solid-set sprinkler irrigation system performance. However, the effect of field boundaries irrigation has not been considered in the whole-field performance. The objectives of this study are 1) to characterize two different solutions to irrigate field boundaries (full circle sprinkler equipped with a deflecting plate, DP, and partial circle sprinklers, PC); 2) to calibrate and validate a ballistic model to adequately simulate these solutions and 3) to analyse the two different designs (DP or PC) from a whole-field perspective. Two types of experiments were designed. The firsts were carried out with an isolated sprinkler under no windy conditions to estimate drop size distribution parameters. The second were performed in a solid-set sprinkler layout under windy conditions to calibrate and validate the ballistic model. The experimental design allows the comparison of both solutions under equal technical and meteorological conditions. Comparisons between designs (DP or PC) were established for a whole field area in terms of irrigation performance and crop yield. From a technical point of view, PC sprinklers perform better than DP sprinklers. From an economical point of view, the shape and orientation of the plot and the legal requirements of the irrigation system design (minimum distance of the sprinkler line to the border) have an important effect on the optimal solution to irrigate field boundaries.

Key words: Sprinkler irrigation, ballistic model, water distribution, field boundaries, sprinkler deflecting plates.

Abbreviations

C	Aerodynamic drag coefficient
C'	Corrected drag coefficient
CUC	Christiansen's uniformity coefficient
D	Drop diameter (mm)
d_1	Large nozzle diameter (mm)
d_2	Small nozzle diameter (mm)
D_{50}	Mean drop diameter (mm)
D_c	Discharge coefficient
DP	Deflecting plate sprinkler
DP_{dw}	Deflecting plate downwind direction
DP_{uw}	Deflecting plate upwind direction
EDP	East deflecting plate
EPC	East partial circle
FC	Full circle sprinkler
ID_e	Emitted irrigation depth (mm)
ID_c	Collected irrigation depth (mm)
K_1, K_2	Empirical parameters
L'	Distance between the nozzle and the impact point with the deflecting plate
n	Dimensionless exponent
P	Operating pressure (kPa)
PC	Partial circle sprinkler
PC_{dw}	Partial circle downwind direction
PC_{uw}	Partial circle upwind direction
Pv	Percent of total sprinkler discharge in drops smaller than D
R	Coefficient of correlation
RMSE	Root mean square error
U	Drop velocity with respect to the ground (m s^{-1})
V	Drop velocity in the air (m s^{-1})
WS	Wind speed (m s^{-1})
WDP	West deflecting plate
WPC	West partial circle
α	Angle formed by the vectors V and W
β	Angle formed by vectors V and U
ρ_a	Air density

1. INTRODUCTION

Solid-set sprinkler systems are commonly used to irrigate crops worldwide. In the literature, numerous researchers have analyzed the solid-set sprinkler system quality (Christiansen, 1942; Keller and Bliesner, 1990; Tarjuelo et al. 1994; Dechmi et al. 2003a; Playán et al. 2005). A specific trait of solid-sets is that irrigation performance heavily depends on meteorological conditions. Wind speed has been shown to reduce irrigation uniformity. In combination with variables such as air temperature, relative humidity, and solar radiation, wind speed also determines wind drift and evaporation losses. In the central Ebro Basin (Spain), Faci and Bercero (1991) recommended users to stop solid-set irrigation for winds exceeding 2 m s^{-1}. Avoiding periods of unfavorable meteorological conditions is a clear target for solid-set irrigation controllers. The performance of sprinkler irrigation depends also on design and operational factors. The most important design factors are the sprinkler type, the use of one or two nozzles, the nozzle diameters, the sprinkler spacing and the design pressure and its variability (Fukui at al. 1980; Kincaid et al. 1996; Playán et al. 2005; Tarjuelo et al. 1999; Zapata et al. 2007). Other works have analyzed the whole-field irrigation performance accounting with operational factors (Mateos 1998) or with pressure variability (Zhang et al. 2013) but the field-boundaries irrigation peculiarity has not been included.

The irrigation of field-boundaries and its effect on the whole field-scale irrigation quality has not been considered. In fact, small field-scale and large sprinkler jet, load to significant losses at the boundaries. These problems can be solved by analyzing different field-boundaries sprinklers solutions and selecting the most appropriate to each situation. Typical solutions for field boundaries can be grouped as: 1) partial (circle) rotation sprinklers PC (commonly located at field-boundaries) or 2) total rotation sprinklers equipped with a deflection plate DP (located several meters away from the field boundaries). The first (PC) has been the most common solution used to irrigate field boundaries in sprinkler irrigated areas all over the word. The second (DP) has been widely installed in the new irrigation modernization projects in Spain, due to the new regulation for the conservation of rural roads and roads. This regulation imposes a minimum distance between the roads and the first sprinkler line of 3 m. Both solutions present different uniformity and cost challenges. The PC sprinklers are typically used at field boundaries, and at standard operation (turn of 180º) affects the half of the area irrigated by a full circle sprinklers (FC). The inconvenient of the PC sprinklers is that its irrigated area was also overlapped by FC sprinklers and the irrigation dose resulted in general larger than the dose from overlapped FC sprinklers. It is very common that irrigated area from overlapped

FC and irrigated area from overlapped PC plus FC take part of the same irrigated block, compromising the irrigation uniformity and the irrigation dose if they are not adequately selected. In plots limiting with roads, public authorities are currently regulating the minimum distance to the first sprinkler line to values ranging from 3 to 8 m from the road side. If the sprinklers of the first line are PC they must be installed at 3 m from the edge and equipped with protective screens. In other cases, they should be placed at a distance not less than the range of the sprinkler to the outer edge of the gutter. In these cases, deflecting plates with different shapes are currently used to curve the sprinkler jet and reduce its throw radius at the deflected orientation.

Computer simulation has proven to be a powerful tool for sprinkler irrigation design and management, due to the large number of involved processes and variables. Sprinkler irrigation system distributes water as discrete drops traveling through the air. Drop characterization is required to estimate the drops falling at a certain distance from the sprinkler. Drop diameter and velocity, as well as their trajectory until reaching the soil surface depend of several factors: type of sprinkler and nozzle, operational hydraulic parameters and environmental conditions where the irrigation sprinkler system is or will be implemented. The ballistic theory has been successfully applied to simulate the landing distance of different drop diameters resulting from a given sprinkler model, nozzle elevation and operating pressure in the absence of wind (Montero et al. 2001; Playán et al. 2006). The ballistic theory considers the wind effect as the main factor of the drops trajectory distortions (Fukui et al. 1980; Playán et al. 2006). Accordingly, a sprinkler is simulated as a device emitting drops of different diameters. It is assumed that drops travel independently from the nozzle until reaching the soil surface. The action of gravity (acting in the vertical direction) and the resistance force (opposite to the drop trajectory) complete the analysis of forces acting on the water drop (Vories et al. 1987; Carrión et al. 2001; Dechmi et al. 2004). According to Fukui et al. (1980) the resistance force of the drop movement can be expressed as:

$$Fr = \frac{1}{8}\rho_a C\pi D^2 V^2 \quad [1]$$

where V is the drop velocity in the air, ρ_a the air density, D the drop diameter and C is a drag coefficient.

The ballistic approach requires a preliminary determination of drop size distribution for a given sprinkler and a set of operating conditions. Li et al. (1994) proposed the following empirical model to fit the drop diameter distribution curve:

$$P_V = \left(1 - e^{-0{,}693\,(\frac{D}{D_{50}})^n}\right) 100 \quad [2]$$

where P_v is the percent of total sprinkler discharge in drops smaller than D, D_{50} the mean drop diameter, and n is a dimensionless exponent. The estimation of the parameters of this equation permits to characterize the drop diameter distribution resulting from a given sprinkler, nozzle diameter and operating pressure.

In order to reproduce the deformation of the circular water application pattern produced by the wind, Seginer et al. (1991) and Tarjuelo et al. (1994) reported on the need to correct the drag coefficient following this expression:

$$C' = C\,(1 + K_1 sen\beta - K_2 cos\alpha) \quad [3]$$

where β is the angle formed by vectors V and U (the drop velocity with respect to the ground), α the angle formed by vectors V and W (the wind vector which is parallel to the ground surface), and K_1 and K_2 are the empirical parameters determined for each wind velocity conditions. Montero et al (2001); Dechmi et al. (2004) and Playán et al. (2006) reported that K_1 and K_2 narrows and displaces, respectively, the water distribution pattern respect to the wind direction. Dechmi et al. (2004) and Playán et al. (2006) used wind-dependent values of both parameters for their particular experimental sprinkler set-up.

Burguete et al. (2007) concluded that the ballistic model, assuming independent movement of the drops formed at the nozzle, constitute an excessive simplification of the reality. These authors reported that group displacement of the drops (jet) results on a reduction of the aerodynamic drag force and in an increased probability of drop collision (resulting in new drop diameters). The authors did not considered aerodynamic resistance in the first 0.5 meter of the trajectory. Within this distance, the jet is compact and is not broken down into drops. Those considerations have improved the ballistic model prediction capability.

The general objective of this paper is to adapt the ballistic model presented by Playán et al. (2006) and modified by Burguete et al. (2007) to simulate the irrigation performance of partial circle sprinkler (PC) and deflection plate sprinkler (DP) and to analyze the differences of both solutions for field-boundaries irrigation. This will be addressed by three specific objectives:

1. On-field experimental characterization of PC and DP performance.
    a. To characterize the irrigation pattern of isolated PC and DP sprinklers under no windy conditions.

b. To characterize the irrigated area of PC and DP as field-boundaries irrigation solutions in a solid-set arrangement.

2. Adaptation, calibration and validation of the ballistic model to adequately simulate the irrigation performance of the two field-boundaries sprinkler solutions.

3. Application of the developed model: To simulate a corn irrigation season of a commercial plot equipped with PC or with DP as boundaries solution. Comparison of simulated results will be established for irrigation performance and corn yield.

2. Material and Methods

2.1. Field experiment

Field experiments designed to evaluate the irrigation performance of agricultural impact sprinklers used for field-boundaries irrigation were conducted at the experimental farm of the Agricultural and Food Research and Technology Centre in Zaragoza, Spain (41◦43'N, 0◦48'W, 225 m altitude) during the years 2011 and 2012. Figure 1a shows the characteristics of the impact sprinklers evaluated in this study: the full circle sprinklers (FC), the partial circle sprinklers (PC) and the full circle sprinkler equipped with a deflection plate (DP). The evaluated FC sprinkler was the RC-130 model (Riegos Costa, Lleida, Spain) equipped with two nozzles (4.4 mm+2.4 mm), while the evaluated PC sprinkler was the RC-135 (Riegos Costa, Lleida, Spain) and was equipped with double nozzle, 3.6 mm + 2.4 mm, PC(2Noz), and with single nozzle 3.6 mm, PC(1Noz). These configurations are widely used in the Ebro Valley (Spain) and in other sprinkler irrigated areas. The deflection plate that was installed to the RC-130 FC model is a commercial prototype (Figure 1b) that has been designed and installed by a company of irrigation engineering with a large tradition in the middle Ebro Valley, Spain. The surface of this deflecting plate is completely plane and was installed parallel to the soil, the principal design characteristics were presented in Figure 1b.

Two types of field experiments were performed, one type was performed using an isolated sprinkler and the other was performed using a rectangular solid-set arrangement.

2.1.1. Isolated sprinkler experiments

Isolated sprinkler experiments were designed to characterize the water distribution pattern of the individual sprinklers and to calibrate the ballistic model parameters in no windy conditions. The experiments were performed on bare soil and under no windy conditions

as specified by the most relevant international standards (ANSI/ASAE 2003; ISO 1990; ISO 1995).

The sprinkler was assembled in a riser tube at 2 m above the ground level (a.g.l). Pluviometers located along radii at distances from the sprinkler ranging from 0.5 to 16.5 m, in increments of 0.5 m, were used to collect the irrigation water. Each pluviometer was 0.40 m high and was conical in shape with a circular opening of 0.16 m located at 0. 5 m a.g.l.. The pluviometers were marked for direct readout with 1 mm intervals of precipitation. Four radii faced north (N), west (W), south (S) and east (E) were used for FC sprinkler experiment (Figure 1a). Three radii, corresponding to W, S and E, were used for PC sprinkler experiment (Figure 1a). Since the jet impacts the paddle holding the deflection plate, one radius of pluviometers faced to the plate was not significant to characterize the radial curve. A special catch can arrangement was required to capture this water application pattern. Catch cans were distributed along 3 radii under the deflecting plate faced North, 30 degree East and 30 degree West (Figure 1a). All the isolated sprinkler experiments were performed for two hours under very low wind conditions. Each sprinkler was tested at three operating pressures: 200, 300 and 400 kPa.

2.1.2. Solid-set experiment

Solid-set experiments were designed to evaluate the irrigation performance using the Christiansen's uniformity coefficient (CUC) and to calibrate and validate the parameter K_1 and K_2 of the ballistic model. In this research the border area of a plot will be considered as a function of the sprinkler type selected to irrigate this area. For plots equipped with PC sprinklers in the edges, the border area corresponds to that overlapped between PC and FC sprinklers (Figure 1a, field arrangement). For plots equipped with DP sprinklers in the edges, the border area corresponds to that between the DP line installation and the edges of the plot (Figure 1a, field arrangement).

Figure 2 shows the experimental plot design. The experimental design permitted to evaluate simultaneously, so under equal technical (pressure) and meteorological (wind) conditions, two different plot-boundaries irrigation solutions (PC and DP) and two jet orientations (West and East) of the plot-boundaries solutions. Experiments were performed under three pressures at the nozzle (200, 300 and 400 kPa), and two levels of wind speed (lower than 2 m s^{-1} and between 2 and 4 m s^{-1}). Due to the relative proximity of the evaluated areas of the different solutions, experiments were only performed for wind speeds lower or equal than 4 m s^{-1} to avoid drift water between experimental areas.

Two zones irrigated by PC sprinklers were selected for evaluation purposes that represent two confronted orientation of the PC sprinkler jet (Figure 2a), East Partial Circle (EPC), and West Partial Circle (WPC). A matrix of 25 pluviometers was installed at 0.50 m a.g.l. in the PC and FC evaluated areas (Figure 2b). Again, two irrigated zones equipped with DP were selected for experiments representing two confronted deflection plate orientations (East Deflection Plate orientation, EDP, and West Deflection Plate orientation, WDP, in Figure 2a). A matrix of 30 pluviometers was installed in DP evaluated areas (Figure 2c) to catch the water distribution variability.

A total of 30 field experiments of solid-set sprinkler irrigation were conducted. Each solid set experiment provides water distribution data for WDP, EDP, WPC, EPD and FC. For each test, the CUC was assessed from the irrigation depth collected (ID_c) in the pluviometers. Experimental comparisons between different solutions were analyzed based on CUC differences for different wind conditions using linear regression analysis.

The wind velocity (WS, m s^{-1}) and direction (WD), the temperature (T) and relative humidity (RH) of the air were monitored by an automatic weather station located in the same plot. The average records were collected every 5 min using a data logger model CR10X (Campbell Scientific Ltd, UK). The operating pressure P (kPa) was monitored at the sprinkler nozzle every 2 minutes by pressure transducers model Dickson PR150 (DicksonWare^{TM} Addison, Illinois, USA). Working pressure was used to compute the gross irrigation water depth emitted by the sprinkler ID_e (mm) at each experiment using the following equation based on the Torricelli's Theorem.

$$ID_e = \frac{0.00035\,\pi D_c\ \overline{P}(d_1^2+d_2^2)\ Te}{S} \quad [4]$$

where D_c is the discharge coefficient (D_c = 0.98 as determined experimentally by Playán et al. 2006); d_1 and d_2 are the large and small nozzle diameter (mm), respectively; P is the pressure at the nozzle (kPa) ; *Te* is the experiment duration (s); and *S* is the area irrigated by one sprinkler (m^2). Playán et al. (2006) calibrated the discharge coefficient equation of the RC130 sprinkler model for various operating pressures by measuring the flow rate in the field.

2.2. Model description, calibration and validation

The ballistic model was used in this study to simulate water distribution patterns of field boundaries sprinkler solutions under different technical and meteorological conditions. To reproduce the functioning of DP sprinklers, the model has been modified to incorporate the

effect of the jet impact with the deflection plate on energy dissipation, drop size distribution and drop trajectories modifications.

The 3D scanner methodology described in Playán et al. (2010) was used to characterize the morphology of the sprinkler jet after the impact and the location of the drops in their trajectory after the plate impact. The 3D scanner was stationed at a distance from an isolated sprinkler of 25 m. In the 3D scanner experiments the sprinkler vertical axis was fixed to avoid rotation, since the sprinkler revolution time (about 30 s) would interfere with the scanning time, which is in the order of minutes (Playán et al. 2010). Although rotation was not permitted, the sprinkler arm oscillated in its normal motion. The ballistic model modified by Burguete et al. (2007) assumed that drops are formed at approximately 0.5 m distance from the sprinkler nozzle. Along this distance, the jet or the drops movement follows the same parabolic trajectory while the resistance force acting on the water drop is considered negligible. Accordingly, the drops velocity can be expressed as:

$$V_z = V_{0z} - gt; \qquad V_x = V_{0x}; \qquad V_y = V_{0y} \qquad [5]$$

where *V* is the drop velocity, V_0 is the initial drop velocity and *t* the time elapsed by the jet travel from the nozzle to the point of break down (where drops are formed) . Therefore, the three directional components of the drop positions are:

$$Z = Z_0 + V_{0z}t - \frac{1}{2}gt^2; \qquad X = X_0 + V_{0x}t; \qquad Y = Y_0 + V_{0y}t \qquad [6]$$

where x, y, z are the coordinates referring to the ground (with origin at the sprinkler nozzle).

In the case of sprinklers equipped with deflection plate, the time elapsed by the jet to impact the plate depends on the height between the nozzle and the plate (*H*):

$$t = \frac{V_{0z} - \sqrt{{V_{0z}}^2 - 2gH}}{g} \qquad [7]$$

A new parameter characterizing the distance between the nozzle and the impact point with the deflecting plate was introduced in the model, L':

$$L' = ({V_{0x}}^2 + {V_{0y}}^2)t \qquad [8]$$

The 3D scanner methodology provides data of the drop trajectory deviation caused by the jet impact that was graphically presented in Figure 3. This figure shows that the majority of drops follow approximately a horizontal movement after the impact. Since drop velocities at the three spatial directions could not be obtained with the 3D scanner method a

simplification has been made, assuming that the energy losses of the impact only modify the vertical component of the velocity, V_z. Assuming this simplification, the component of the drop velocity after the jet impact can be expressed as:

$$V_z = 0; \qquad V_x = V_{0x}; \qquad V_y = V_{0y} \qquad [9]$$

It is assumed that drops travel independently until reaching the soil surface after the decomposition of the jet due to the resistance forces, or after the impact with the deflecting plate. At this point, ballistic theory is used to determine the trajectory of each drop diameter subjected to an initial velocity vector and a wind vector. The calibration process of the ballistic model reported by Playán et al. (2006) has been used in this research. The methodology has two steps. The first step consisted on fitting the drop diameter distribution curve parameters, D_{50} and n (Eq. [2]), to reproduce the radial water distribution pattern in the absence of wind. Isolated field experiment data were used to calibrate these parameters. Two statistical indexes were used to compare measured and simulated water application patterns: the Root Mean Square Error (*RMSE*) and the coefficient of correlation (r). These two statistical indexes were based on water depths at sampling locations. An automatic calibration process was developed and incorporated to the ballistic model. The Monte-Carlo computational algorithm (Fishman, 1995) was used for the optimization of the calibration process. This method is a brutal force algorithm that calculates the values of the calibration parameters with pseudo-random numbers obtained from established ranges. Although the method has a slow convergence, is very robust and it does not remain in local minimum values (Burguete and Latorre 2014). The ratio $RMSE/(1+r)$ were used as the objective function for the optimization algorithm.

The second step of the calibration process consists on fitting the values of parameters K_1 and K_2. Experimental solid-set water distribution patterns under different wind conditions were used for this second step. The dominant wind speed and wind direction (Sanchez et al., 2011b) were determined for each irrigation event in order to incorporate it into the model. The comparison between measured and simulated water depths at the measurement points was established in terms of the two above-mentioned indexes (*RMSE* and r) and the ratio between them. As a confirmation of the calibration results, the absolute difference between observed and simulated CUC (ΔCUC, %) was also obtained. The same automatic calibration process reported before was also used to calibrate the values of K_1 and K_2 parameters.

To select the optimum K_1 and K_2 values, a total of 121 simulations were performed with K_1 values ranging from 0.0 to 2.7 (with an increment of 0.3) and K_2 values ranging from 0.0 to

1.0 (with an increment of 0.1) for FC and PC sprinklers. For DP arrangement experiments a total of 300 simulations were performed, with the value of K_1 and K_2 ranging from 0.0 to 5.0 for each experiment.

For PC sprinkler calibration and validation processes, the values of the model parameters for FC sprinklers that overlapped with PC were fixed previously.

The model validation consisted on comparing measured and simulated irrigation depth for the irrigation experiments reserved for validation purposes and not used for calibration. The validation experiments permits to evaluate the capacity of the model to reproduce irrigation events in technical and meteorological conditions different from the ones used for calibration but in the same range. From the 30 solid-set experiments, 24 were used for model calibration of K_1 and K_2, and 6 were reserved for model validation.

2.3 Model applications

The differences in irrigation performance and corn yield of a commercial plot designed with three different solutions for the plot-boundaries irrigation were simulated. The three designs were: 1) using PC(1Noz) as plot-boundaries sprinklers; 2) using PC(2Noz) as plot-boundaries sprinklers; or 3) installing DP as plot-boundaries sprinklers. The central area for the three designs was equipped with the FC sprinkler studied in this research. The plot has a total area of 12 hectares arranged in an elongated and narrow shape that gives it a high edge surface. The irrigation system in all the three cases was divided in 12 irrigation blocks, all with a part of boundaries sprinklers. The irrigation schedule of a corn crop was computed according to the crop water requirements provided by the Irrigation Advisory Service of the plot location for 2008 irrigation season. The irrigation schedule was simulated for all irrigation designs, considering similar meteorological conditions for all the irrigated blocks. Comparisons were established in terms of volume of irrigation applied and on irrigation uniformity. The simulated irrigation depth for each irrigation system design and for each irrigation event was coupled with Ador-Crop (Dechmi et al. 2004) a crop simulation model to simulate corn yield. Ador-Crop was calibrated and validated by Dechmi et al. (2004) and was used by Zapata et al. (2009) and Zapata et al. (2013) to simulate corn yield in the same irrigated area. Comparisons between whole-field irrigation designs were also established in terms of corn yield.

3. Results and discussions

3.1. Isolated sprinkler experiment: Calibration of D_{50} and n.

For PC and FC sprinklers the radial curve was obtained selecting the most adequate experiment and averaging the three or four radii of the selected experiment, respectively. Figure 4 shows the experimental water distribution pattern (solid line) and the simulated water distribution pattern (dashed line) for the four evaluated sprinklers at 200, 300 and 400 kPa operating pressure. The Figure 4 also showed for each selected experiment the standard deviation of the three or four radii. For a given operating pressure, the radial curve of the FC sprinkler (Figure 4a, 4b and 4c) was more similar to the PC(1Noz) sprinkler (Figure 4d, 4e and 4f) than to the PC(2Noz) sprinkler (Figure 4g, 4h and 4i), both in shape and in the total volume of water applied. Therefore, from the point of view of water applied and under no wind conditions, overlapping the FC sprinklers with the PC(1Noz) would be the best alternative to irrigate field boundaries. The radial water distribution noticeably differed between PC(1Noz), PC(2Noz) and DP sprinklers. The PC(2Noz) distributed more water in the first 7 meters from the sprinkler compared with the PC(1Noz). Figures 4j, 4k and 4l show the shape of the radial curves for the DP sprinkler for the deflected radii and for the no deflected radii. For the deflected radii most of the water is applied in the first 6 meters, while the water distribution in the no deflected radii was the FC radial water distribution. The water distribution in a solid-set spacing depends greatly on the shape of the radial water distribution curve of the sprinkler selected. Tarjuelo et al. (1999) reported that the shape of the radial water distribution curve is mainly determined by the sprinkler model and its internal design, the discharge angle and by the jet break-up mechanism of the sprinkler. Several authors have reported the need that the information of the standard radial water distribution of sprinklers should be included in sprinkler technical information since this information is important for an optimum sprinkler system design (Sánchez et al. 2011; Stambouli et al. 2013). This is especially important for field-boundaries irrigated areas where the overlapping of different sprinkler is very common. The radial water distribution of the overlapped sprinklers should be similar to obtain adequate irrigation performance.

For the FC and PC sprinkler experiments, a range of D_{50} and n pairs of values were explored (D_{50} from 0.0010 to 0.0020 m, with an increment of 0.0001 m; n from 1.5 to 3.0, with an increment of 0.15). The range was selected following Playán et al. (2006). For DP sprinkler experiments, a wide range of D_{50} and n pairs of values were explored (D_{50} from 0.0005 to 0.0050 m, with an increment of 0.0001 m; n from 1 to 5.0, with an increment of 0.01), to analyze the effect of jet deflection on drop size distribution. The calibration process of the drop size distribution parameters was performed using the automatic calibration tool.

The results of the calibrated parameters are presented in Table 1. In general, the correlation coefficient between measured and simulated water depths was very high (average of r = 0.94), with the lowest value corresponding to the DP sprinkler (r = 0.81). *RMSEs* between measured and simulated radial water application depths ranged from 0.28 to 2.13 mm h^{-1}, with an average value of 1.00 mm h^{-1}. Again, the largest *RMSE* correspond to the DP sprinkler. The statistical parameters showed the adequate capacity of the model to simulate and reproduce the radial water distribution pattern of the evaluated isolated sprinklers (Figure 4).

The FC sprinkler analyzed in this research was also analyzed by Playán et al. (2006). Values of D_{50} and n parameters resulted slightly different and the statistics of the new parameters improve the simulation results. The differences could be mainly attributed to model definition since in this research the improvements presented in Burguete et al. (2007) has been incorporated to Playán et al. (2006) model. On the other hand the automatic optimization model permits easily amplify the range of values for the parameters and could also contribute to the improved results.

Figure 5 presents simulated 3-D water distribution patterns for FC, PC(1Noz), PC(2Noz) and DP sprinklers operating at 300 kPa. The effect of the deflection plate on the water distribution is well represented showing the high volume of water applied in a reduced area, not exceeding 6 meters from the sprinkler for this particular plate design and location

3.2. Solid-set sprinkler experiment: Calibration of K_1 and K_2 parameters.

In field experiments, the range of wetted diameter of DP sprinklers does not exceed 6 meters from the sprinkler, in the direction of the deflected jet. In DP cases the calculations of uniformity have been performed considering a maximum throw distance of 6 meters in the deflected direction. The emitted irrigation depth (ID_e) around the field-boundaries irrigated by DP sprinklers is 50% higher than that applied by the FC sprinklers; the reduction of the considered irrigated area for DP greatly increased the ID_e. The ID_e and ID_c at the FC irrigated area were considered as the reference for comparison. The ID_e of the PC sprinklers is 1.7% and 24.5% higher than that of the FC sprinklers, for PC(1Noz) and PC(2Noz), respectively.

A significant variation of collected irrigation depth, ID_c, was measured between the central area (FC zone) and the field-boundaries areas, and the differences were function of wind speed and wind direction. Average ID_c at FC (4.7 mm h^{-1}) zone was higher than the ID_c PC(1Noz) averaging 19% for the downwind direction (PC_{dw}) and 8% for the upwind direction (PC_{uw}), although ID_e for PC(1Noz) was slightly higher. In the case of PC(2Noz),

ID_c was quite similar to ID_c at the FC zone for downwind direction and slightly larger (6%) for upwind direction.

The magnitude of differences of ID_c between the FC zone and the DP zones was greatly affected by the relative direction of wind to the sprinkler jet trajectory. For wind direction upward DP orientation (DP_{uw}), the ID_c of DP resulted in average 3.5% lower than the ID_c of FC. For wind direction downward DP (DP_{dw}) orientation, the ID_c of DP resulted in average 39% higher than the ID_c of FC.

The wind speed in the field experiments varied between 0.5 and 3.36 m s^{-1}. The performance parameter CUC of the solid set evaluations showed an ample range of variation. In calm conditions (wind speed < 1 m s^{-1}) and for the FC sprinkler experiments, the CUC ranged from 84% to 93%, while in windy conditions (wind speed > 1 m s-1) the CUC ranged from 62% to 94%. The wind speed has been reported by several authors (Christiansen 1942; Seginer et al. 1991; Tarjuelo et al. 1999; Playán et al. 2005) as the most environmental factor affecting sprinkler irrigation performance. The effect of the direction of the wind respect to the jet orientation is larger in the irrigation performance of DP sprinklers than in PC sprinkler (Figure 6). Differences on CUC between FC and DP are relevant (>20%) under low wind conditions, increases with wind speed and upwind direction (FC-DP_{uw}) and decreases with wind speed and downwind direction (FC-DP_{dw}), for wind speeds larger than 1 m s^{-1}. Similar behavior and values of the differences were observed for the comparison between PC(1Noz) and DP (Figure 6b). Differences on CUC between FC and PC(1Noz), showed in Figure 6c, were almost 0 under low wind conditions and slightly increases with wind speed and downwind direction (FC-PC_{dw}(1Noz)) and slightly decreases with wind speed and upwind direction (FC-PCu_w(1Noz)). The comparison of CUC between FC and PC(2Noz) showed similar trend than the previous one, PC(1Noz), but the values of the differences are slightly larger.

The experimental results indicate that for field-boundaries sprinklers K_1 and K_2 parameters should be obtained as a function of wind direction related with the jet orientation. Two cases were considered, upwind direction (DP_{uw} and PC_{uw}) and downwind direction (DP_{dw}, PC_{dw}).

Tables 2, 3 and 4 present the technical (pressure) and meteorological (average and predominant wind speed and direction) conditions of the solid-set field experiments for the FC, PC(1Noz and 2Noz) and DP sprinklers, respectively. For PC (Table 3) and DP (Table 4) results were organized as downward wind direction and upward wind direction. The tables also show the experimental CUC (CUC_e), the difference between measured and simulated CUC (ΔCUC), the calibration and validation parameters of wind pattern

distortion (K_1 and K_2) and the statistics of the calibration and validation process (*RMSE* and *r*). A column of the three tables called “Use”, classify the experiments in calibration (*c*) and validation (v) experiments.

For FC sprinklers, the optimum K_1 and K_2 parameters reported *RMSE* (of ID_c) values ranging from 0.70 mm h^{-1} to 1.80 mm h^{-1}, with an average of 1.08 mm h^{-1}. The correlation coefficient ranged from 0.16 to 0.82, with an average of 0.54. The lowest correlation coefficients correspond to high uniformities (CUC >83%). Similar results were found by Playán et al. (2006) using the same FC sprinkler working at similar conditions. The absolute differences between experimental and simulated uniformity (∆CUC, %) were very low, ranging from 0.0% to 5.0% (Table 2), showing the adequacy of the model to predict CUC in different technical and meteorological conditions.

For PC(1Noz) sprinklers, the correlation coefficient ranged from 0.20 to 0.86, with an average of 0.52, while the *RMSE* ranged from 1.20 to 2.13mm h^{-1}, with an average of 1.48 mm h^{-1}. For PC(2Noz) sprinklers, the *r* coefficient ranged from 0.17 to 0.91, with an average of 0.62, while the *RMSE* ranged from 1.59 to 2.60 mm h^{-1}, with an average of 1.68 mm h^{-1}. Moreover, the ∆CUC (%) were relatively moderate ranging from 0.0% to 8.0% (Table 3), with an average value of 2.7%. The lowest correlation coefficients and largest *RMSE* correspond to the highest evaluated uniformities (CU > 78%). In these irrigation events the variability in irrigation depth is moderate and the experimental error may account for a large part of the variability.

Table 3 presents the K_1 and K_2 calibrated parameter for the PC(1Noz) and PC(2Noz). As reported before, the analysis has been performed for two relative orientations, downwind and upwind, and for the three working pressures. In general (except for punctual cases), K_1 and K_2 parameters increase with wind speed, the effect of working pressure on them were not clear and neither the effect of PC configuration, 1Noz and 2Noz. To extend the values of K_1 and K_2 parameters for non-evaluated conditions, linear interpolation between the two nearest neighbors were used.

Table 4 presents the K_1 and K_2 calibrated and validated parameters for the DP sprinkler. Again, the analysis has been performed for two relative orientations, downwind and upwind, and for the three working pressures. The *r* coefficient ranged from 0.37 to 0.96, with an average of 0.80, while the *RMSE* ranged from 1.24 mm h^{-1} to 4.38 mm h^{-1}, with an average of 2.19 mm h^{-1}. The ∆CUC (%) ranged between 0.0% and 25.0%. The highest ∆CUC (25.0%) values were obtained in DP_{uw}. The *RMSE* resulted higher than those obtained for PC or FC sprinklers, although the correlation coefficients were the highest. Part of the errors could be attributed to the simplification of wind speed orientation related

with the deflected jet orientation that in this study has been reduced to upward and downward wind direction. Also, the model assumes that the energy losses of the jet impact with the plate only modify the vertical component of the velocity, V_z, since the other velocity components could also be modified. In a further research, measurements of drops velocity after the impact will provide data to estimate modifications of all the drop velocity components and trajectories.

The measured CUC of DP_{dw} under no windy conditions resulted lower than the CUC of DP_{dw} under moderate wind conditions (Table 4). This behavior was not the case for DP_{uw} which CUC decreases as wind speed increases, as do K_1 parameters for this sprinkler configuration and orientation. The rest of parameters showed a general increase with wind speed. The effect of the working pressure on parameter values was not clear. In general, the values of the K_1 parameter for DP resulted larger than those for PC and FC. As for PC, values of K_1 and K_2 for the validation cases of DP were obtained by linear interpolation from the two nearest neighbors.

In general, K_2 was much less relevant than K_1, as reported by Montero et al. (2001). Tarjuelo et al. (1994) identified a different relationship between the magnitude of the correction parameters and the wind speed. Montero et al. (2001), in their calibration of the SIRIAS model, found no relationship between wind speed and the magnitude of the correction parameters. The wide range of variation of the optimum values of K_1 and K_2 point out the poor physical basis of the drag coefficient function. In fact, these parameters have poor physical meaning. This could be explained by the complicated effect of the aerodynamic shielding produced by the grouped drops movement, and especially at the beginning of the trajectory. Nevertheless, until today there is no better model to approximate the effects of wind in sprinkler irrigation.

Figure 7a presents the comparison of CUC experimental (CUC_e) versus CUC calibrated (CUC_c) for the FC, PC and DP sprinklers (different symbols were used for each sprinkler type). Regression lines were established forcing to 0 the origin coordinate and the correlation coefficients were R^2 = 0.92, R^2 = 0.88 and R^2 =0.98 for FC, PC and DP sprinklers, respectively. The regression slope was not significantly different from 1 at the 95% probability level. The CUC was accurately predicted with a standard error of 2.21%, 3.73% and 3.62% for FC, PC and DP sprinklers, respectively. The model shows a good predictive capacity to simulate the CUC in calm and moderate wind conditions and for the two sprinklers types used as solution for field-boundaries irrigation.

3.3. Model validation

The model was validated with data from the series of experiments in calm and windy conditions not used for the calibration process. The validation experiments were presented at the Use column in Table 2, 3 and 4 with a *v* value. In general, the comparison between water depths measured and simulated in terms of *r* and *RMSE* coefficients resulted similar for the validation experiments and for the calibration experiments.

Figure 7b shows a scatter plot of experimental versus simulated CUC for the validation experiments (CUC_v) of FC, PC and DP sprinklers (different symbols were used for each sprinkler type). The regression analysis for the validation experiments proved a significant relationship with a correlation coefficient of $R^2 = 0.91$, $R^2 = 0.82$ and $R^2 = 0.64$ for FC, PC and DP sprinklers. The regression slope and the intercept were not significantly different from 1 and 0, respectively, at the 95% probability level for FC and PC sprinklers but was different for DP sprinkler. The standard errors of CUC estimation were 1.65%, 3.55% and 5.07% for FC, PC and DP experiments. Comparison between experimental (left side figures)and model simulations (right side figures) water distribution patterns was presented in Figure 8 for PC(1Noz) and DP sprinklers for downward and upward wind orientations. The figures showed that the model not only provides a good estimation of CUC parameter but also the water distribution pattern was also adequately simulated.

Irrigation with PC sprinklers provides higher uniformities than with DP sprinklers under low wind speed conditions. For moderate wind speed conditions the results were highly dependent on wind direction orientation respect to the jet. In these irrigation events the variability in irrigation depth is moderate and the experimental error may account for a large part of the variability. Correlation coefficients resulted higher for DP than for PC, although *RMSE* resulted larger for DP than for PC. Operating pressure, nozzle diameter, and sprinkler arrangement respect to the dominant winds did not appear to influence model accuracy. The most innovative aspect of the proposed model is that water application and water uniformity can be determined for a whole field irrigated simultaneously with full circle solid-set sprinklers and boundaries sprinklers (FC with PC sprinklers, or FC with DP sprinklers). The model showed a reasonable predictive capacity to simulate drop water movement affected by the deflecting plate and high windy conditions. The model has the capacity to simulate the water distribution pattern for DP sprinklers equipped with different deflecting plate shapes and under different weather conditions.

3.4 Model applications: Comparison between PC and DP as plot-boundaries irrigation solutions.

The irrigation system of the commercial plot presented in Figure 9 was designed using as plot-boundaries irrigation solutions: 1) PC(1Noz), 2) PC(2Noz) or 3) DP. For designs 1 and 2, the total number of sprinklers was 432, being 122 PC sprinklers (Figure 10). When the plot-boundaries irrigation solution was DP the total number of sprinklers was reduced to 390 (9.7% lower), being 113 DP. The investment cost of designs 1 and 2 were 3,000 € ha^{-1}, the cost of design 3 was 2,900 € ha^{-1}. In this work the cost of DP sprinkler was similar to PC sprinkler.

The irrigated area affected by PC sprinkler for designs 1 and 2, PC(1Noz) and PC(2Noz), respectively, was 32.8% of the total area. In design 3, DP irrigated area accounted for only 10.2% of the total area.

Table 5 presents the simulation results for the three evaluated designs. The first part of the table shows the simulated results for the area irrigated under each specific sprinkler type and orientation. The second part of the table presents the simulation results for the whole-field area under the three different designs.

As reported before, and due to the characteristic plot shape (Figure 9) all the irrigation blocks had FC sprinklers and plot-boundaries sprinklers that irrigates at the same time. The total irrigation time scheduled was 123 hours, arranged in 28 irrigation events, averaging 4.4 hours per irrigation event. The inner irrigated area equipped with FC sprinklers applied a seasonal irrigation depth of 641 mm (6410 m^3 ha^{-1}), similar to that applied by PC(1Noz), 652 mm. At the DP area, the applied seasonal irrigation depth is the highest, 975.4 mm, since the half of the sprinkler discharge was spread in a reduced area of 18 m x 6 m. Although the irrigation uniformity of the DP area was the lowest its high irrigation dose smooth the effect on corn yield.

The simulation results presented in Table 5 indicated that the differences in corn yield were negligible (<1%) although the seasonal applied irrigation depths were slightly different between plot-boundaries irrigation solutions (<7%). The lowest seasonal applied irrigation depth (644 mm) for the total plot area corresponds to design 1, with PC(1Noz) as plot-boundaries irrigation solution. The largest seasonal depth (693 mm) corresponds to design 2 with PC(2Noz) as plot-boundaries irrigation solution. The intermediate value corresponds to the plot-boundaries design with DP sprinklers (675 mm). From a technical point of view, PC sprinklers perform better than DP sprinklers. When analyzing the total area of the commercial plot presented in Figure 9, differences between PC(1Noz) and DP in investment cost (4% larger for PC(1Noz)) and water applied (5% larger for DP) results in similar net income for both solutions. The analysis has been performed for the 2008 irrigation season that could be classified as an average meteorological season in the area.

For plot shapes with lower edge surfaces, the difference in investment cost could not equilibrate the difference in water applied and exploitation cost. In this case, the best solution was PC sprinklers.

4. Conclusions

1- The sprinkler jet orientations respects to the wind direction have a clear effect on the irrigation uniformity of field-boundaries sprinklers under windy conditions, especially in deflecting plate sprinklers. In areas with frequent and predominant wind directions, DP sprinklers (as a field-boundaries solution) could be installed in the field-boundaries where the deflected jet trajectory was going upwind. In any other boundaries, the DP solutions will lead to mediocre results.

2- The experimental comparison showed that in windy conditions, PC field-boundaries sprinkler (single or double nozzles) performs better than DP field-boundaries sprinkler.

3- New considerations and process have been introduced in the ballistic model to simulate field-boundaries sprinklers such as, the effect of the movement of drops in groups on the aerodynamic drag forces, the deflecting plate effect on the drops movement and the use of the Monte-Carlo method to generate different drop diameters. The model shows potential to become a valuable tool to manage solid-set sprinklers irrigation under different technical and meteorological conditions.

4- The calibrated model has reproduced accurately the water distribution pattern (r = 0.94, $RMSE$ = 1 mm h^{-1}) for different sprinklers types; FC, PC and DP sprinklers. The resulting ballistic model has proven to have a satisfactory predictive capacity of CUC. The calibration and validation standard errors for CUC were 3.46% and 4.35%, respectively.

5-

Comparisons between field-boundaries design solutions were established for the whole field area in terms of irrigation performance and crop yield. Differences in corn yield were negligible (<1%) although the seasonal applied irrigation depths were slightly (<7%) different between field-boundaries irrigation solutions. Analyzing investment cost, exploitation cost (water applied and associated energy) and corn crop income, DP solution could be an alternative to PC when the shape of the plot is long and narrow and the border area represents a high percentage of the total plot area.

Acknowledgements

This paper applies the “first-last-author-emphasis” approach for the sequence of authors. This research was funded by the MCINN of the Government of Spain through grants AGL2010-21681-C03-01, AGL2013-48728-C2-1-R and the FPI MINECO PhD grants program. The authors would like to thank the CITA/CSIC field staff and technicians: Miguel Izquierdo, Jesús Gaudó and Ricardo Santaolaria.

REFERENCES

ANSI/ASAE (2003) Procedure for sprinkler distribution testing for research purposes. ANSI/ASAE S330.1, St. Joseph, MO USA

Burguete J, Playán E, Montero J, Zapata N (2007) Improving drop size and velocity estimates of an optical disdrometer: implications for sprinkler irrigation simulation. ASABE 50(6): 2103-2116

Burguete J, Latorre B (2014) Calibrator: A software to perform calibrations of empirical parameters. URL https://github.com/jburguete/calibrator

Carrión P, Tarjuelo JM, Montero J (2001) SIRIAS: a simulation model for sprinkler irrigation. Description of model. Irrigation Science 20: 73–84

Christiansen JE (1942) Irrigation by sprinkling. University of California Aricultural Experimental Station. Bulletin 670

Dechmi F, Playán E, Faci J, Tejero M (2003a) Analysis of an irrigation district in northeastern Spain. I: Characterisation and water use assessment. Agric. Water Manage 61: 75–92

Dechmi F, Playán E, Cavero J, Martínez-Cob A, Faci JM (2004) A coupled crop and solid set sprinkler simulation model: I. Model development. Journal of Irrigation and Drainage Engineering, ASCE 130(6): 499-510

Faci JM, Bercero A (1991) Efecto del viento en la uniformidad y en las pérdidas por evaporación y arrastre en el riego por aspersión. Investigación Agraria. Producción y Protección Vegetales 6(2) (In Spanish)

Fishman, GS (1995) Monte Carlo: Concepts, Algorithms, and Applications. New York: Springer, pp 621. ISBN 0-387-94527-X

Fukui Y, Nakanishi K, Okamura S (1980) Computer evaluation of sprinkler irrigation uniformity. Irrigation Science 2: 23–32

ISO (1990) Agricultural irrigation equipment. Rotating sprinklers. Part 2. Uniformity of distribution and test methods. ISO Standard 7749/2, Geneve

ISO (1995) Agricultural irrigation equipment. Rotating sprinklers. Part 1. Design and operational requirements. ISO Standard 7749/1, Geneve

Keller J and Bliesner R D (1990). Sprinkle and trickle irrigation. Van Nostrand Reinhold, New York, NY. 652 pp

Kincaid DC, Solomon KH, Oliphant JC (1996) Drop size distributions for irrigation sprinklers. Trans. ASAE 39(3): 839-845

Li J, Kawano H, Yu K (1994) Droplet size distributions from different shaped sprinkler nozzles. Trans. ASAE 37(6): 1871-1878

Mateos L (1998) Assessing whole-field uniformity of stationary sprinkler irrigation systems. Irrig Sci 18:73–81

Montero J, Tarjuelo JM, Carrión P (2001) SIRIAS: a simulation model for sprinkler irrigation: II. Calibration and validation of the model. Irrig. Sci. 2001 (20): 85–98

Playán E, Salvador R, Faci JM, Zapata N, Martínez-Cob A, Sánchez I (2005) Day and night wind drift and evaporation losses in sprinkler solid-sets and moving laterals. Agric. Water Manage 76(3): 139–159

Playán E, Zapata N, Faci JM, Tolosa D, Lacueva JL, Pelegrín J, Salvador R, Sánchez I, Lafita A (2006) Assessing sprinkler irrigation uniformity using a ballistic simulation model. Agricultural Water Management 84: 86–100

Playán E, Zapata N, Burguete J, Salvador R, Serreta A (2010) Application of a topographic 3D Scanner to irrigation research. Irrig. Sci 28(3):245-256

Sánchez I, Faci JM, Zapata N, Martínez-Cob A (2011) The spatial variability of the wind in a sprinkler irrigated district: Implications for irrigation management. Biosystem Engineering I(09): 65-76

Seginer I, Kantz D, Nir D (1991) The distortion by wind of the distribution patterns of single sprinklers. Agric. Wat. Manag. 19: 314-359

Stambouli T, Zapata N, Faci JM (2013) Performance of new agricultural impact sprinkler fitted with plastic nozzles. Biosystems Engineering 118: 39-51

Tarjuelo JM, Carrión P, Valiente M (1994) Simulación de la distribución del riego por aspersión en condiciones de viento. Investigación Agraria, Producción y Protección Vegetal 9: 255-271

Tarjuelo JM, Montero J, Carrión PA, Honrubia FT, Calvo A (1999) Irrigation uniformity with medium size sprinklers part II: influence of wind and other factors on water distribution. Transactions of the ASAE, 42(3): 677-690

Vories ED, Von Bernuth RD, Mickelson RH (1987) Simulating sprinkler performance in wind. J. Irrig. Drain. Eng. 113(1): 119-130

Zapata N, Playán E, Martinez-Cob A, Faci JM, Lecina S (2007) From on-farm solid-set sprinkler irrigation design to collective irrigation network design in windy areas. Agric. Water. Manage. 87 (2): 187-199

Zapata N, Playán E, Skhiri A, Burguete J (2009) Simulation of a Collective Solid-Set Sprinkler Irrigation Controller for Optimum Water Productivity. J Irrig Drain Eng ASCE. 135 (1): 13-24

Zapata N, Salvador R, Cavero J, Lecina S, López C, Mantero N, Anadón R, Playán E (2013) Field test of an automatic controller for solid-set sprinkler irrigation. Irrig. Sci 31(5): 1237-1249

Zhang L, Merkley GP, Pinthong K (2013) Assessing whole-field sprinkler irrigation application uniformity. Irrig. Sci 31: 87-105

LIST OF FIGURES

LIST OF TABLES

Table 1. Results of the calibration parameters D_{50} and n for the drop size distribution model.

Sprinkler	Nozzle diameter (mm)	Nozzle Pressure (kPa)	Discharge (l s^{-1})	D_{50} (mm)	*n*	*RMSE* (mm h^{-1})	*r*
	4.4+2.4	200	0.38	1.70	2.25	0.28	0.99
FC	4.4+2.4	300	0.47	1.40	2.25	0.49	0.98
	4.4+2.4	400	0.54	1.30	2.25	0.48	0.98
	3.6	200	0.20	1.60	2.00	0.57	0.96
PC(1Noz)	3.6	300	0.24	1.50	2.30	0.28	0.99
	3.6	400	0.28	1.52	2.20	0.41	0.98
	3.6+2.4	200	0.29	1.40	2.00	0.65	0.98
PC(2Noz)	3.6+2.4	300	0.35	1.30	2.10	1.54	0.96
	3.6+2.4	400	0.40	1.20	2.20	1.44	0.96
	4.4+2.4	200	0.38	1.00	1.66	1.78	0.84
DP	4.4+2.4	300	0.47	1.00	2.38	2.01	0.81
	4.4+2.4	400	0.54	1.00	2.56	2.13	0.82

Table 2. Field experimental conditions for the FC sprinklers evaluations. Results of the field experiments, model parameters and statistics between measured and simulated water distribution patterns were presented.

Pressure (kPa)	WS ($m\ s^{-1}$)	Predom. WS ($m\ s^{-1}$)	Dir.	Use	FC					
					CUCe (%)	ΔCUC (%)	K_1	K_2	RMSE	r
200	0.64	0.39	SE	c	84	4	0.0	0.0	1.04	0.16
	0.65	0.52	NNW	c	87	0	0.0	0.0	1.06	0.27
	1.09	1.02	N	c	88	2	0.0	0.1	0.87	0.43
	1.19	1.16	NNW	v	84	2	0.3	0.2	0.87	0.43
	1.57	1.43	ESE	v	82	2	0.8	0.3	0.74	0.65
	1.62	1.51	SE	c	86	3	0.9	0.3	0.74	0.65
	2.51	2.06	WNW	c	78	2	1.8	0.4	1.22	0.57
	2.60	2.4	WNW	c	79	3	1.8	0.4	1.31	0.52
	3.27	3.25	W	c	62	1	1.2	0.6	1.43	0.65
	3.36	3.31	W	c	72	2	1.2	0.6	1.03	0.75
300	0.52	0.35	SE	c	88	2	0.0	0.0	0.70	0.60
	0.61	0.35	S	c	92	2	0.0	0.0	0.70	0.40
	1.00	0.8	ENE	c	94	5	0.0	0.1	0.82	0.16
	1.25	1.22	SSE	v	92	4	0.0	0.1	1.02	0.48
	1.54	1.45	SE	v	88	2	0.0	0.1	0.90	0.27
	1.70	1.66	N	c	88	0	0.0	0.1	0.77	0.68
	2.40	2.27	W	c	79	1	1.2	0.3	1.35	0.81
	2.40	2.32	WSW	c	78	0	1.2	0.3	1.46	0.61
	2.71	2.67	WSW	c	78	0	0.9	0.3	1.48	0.48
	3.09	3.04	WSW	c	76	1	0.9	0.3	1.02	0.79
400	0.50	0.18	NE	c	91	1	0.0	0.0	0.84	0.42
	0.61	0.36	NNE	c	93	2	0.0	0.0	0.71	0.25
	1.21	0.96	S	c	92	2	0.0	0.1	1.05	0.47
	1.36	1.23	S	v	89	0	0.0	0.1	1.11	0.54
	1.59	1.35	WSW	v	87	2	0.0	0.1	0.95	0.52
	1.62	1.59	SSE	c	88	0	0.0	0.1	1.08	0.68
	3.10	2.3	W	c	83	3	1.2	0.4	1.80	0.54
	3.13	3.1	W	c	74	1	1.2	0.4	1.56	0.82
	3.18	2.98	WNW	c	78	0	1.2	0.3	1.36	0.78
	3.21	3.18	W	c	66	5	1.2	0.3	1.44	0.77

Table 3. Field experiment conditions for the PC(1Noz) and PC(2Noz) solid-set evaluations arranged in downwind (PC_{dw}) and upwind (PC_{uw}) orientations. Experimental results, calibrated and validated parameters and statistics between measured and simulated water distribution patterns were also presented.

Press. (kPa)	Predom. WS ($m\ s^{-1}$)	Dir.	Use	PC_{dw} (1Noz)						PC_{uw} (1Noz)					
				CUCe (%)	ΔCUC (%)	K_1	K_2	RMSE	r	CUCe (%)	ΔCUC (%)	K_1	K_2	RMSE	r
200	0.52	NNW	c	78	8	0.0	0.0	1.20	0.31	84	6	0.0	0.0	1.06	0.2
	1.02	N	c	81	3	0.0	0.8	1.60	0.22	75	4	0.0	0.7	1.53	0.33
	1.16	NNW	v	71	0	0.0	0.8	1.67	0.35	75	2	0.1	0.7	1.61	0.3
	3.25	W	c	54	0	0.3	0.5	1.45	0.71	63	6	1.2	0.7	1.21	0.84
	3.31	W	c	60	1	0.3	0.5	1.55	0.58	69	1	1.2	0.7	1.03	0.77
300	0.35	SE	c	85	4	0.0	0.0	1.24	0.32	83	3	0.0	0.0	1.08	0.45
	1.45	SE	c	80	2	0.0	0.6	1.61	0.31	84	1	0.3	0.4	1.25	0.45
	1.66	N	v	79	1	0.1	0.5	1.81	0.51	79	1	0.5	0.4	1.37	0.59
	2.67	WSW	c	65	2	0.6	0.2	2.13	0.31	75	0	1.5	0.5	1.40	0.77
	3.04	WSW	c	62	1	0.6	0.2	1.18	0.86	74	1	1.5	0.5	1.00	0.86
400	0.36	NNE	c	86	3	0.0	0.0	1.40	0.48	89	3	0.0	0.0	1.27	0.41
	1.35	WSW	c	79	1	1.2	0.0	1.76	0.41	83	7	0.6	0.4	1.29	0.57
	1.59	SSE	v	80	0	1.5	0.2	1.52	0.68	85	1	0.8	0.4	1.65	0.35
	2.30	W	c	68	7	2.4	0.8	2.00	0.55	75	6	1.2	0.5	2.09	0.77
	2.98	WNW	c	65	5	2.4	0.8	1.48	0.69	76	1	1.2	0.5	1.90	0.73
				PC_{dw} (2Noz)						PC_{uw} (2Noz)					
200	0.39	SE	c	82	4	0.0	0.0	1.59	0.37	79	5	0.0	0.0	1.31	0.38
	1.43	ESE	c	78	0	0.0	0.7	1.60	0.17	72	1	0.6	0.3	1.57	0.67
	1.51	SE	v	81	5	0.1	0.7	1.25	0.47	76	5	0.5	0.4	1.45	0.72
	2.06	WNW	c	78	2	0.9	0.8	1.50	0.17	74	1	0.0	0.7	1.60	0.71
	2.40	WNW	c	74	4	0.9	0.8	1.10	0.66	70	2	0.0	0.7	1.90	0.60
300	0.35	S	c	86	6	0.0	0.0	1.51	0.64	83	5	0.0	0.0	1.51	0.65
	0.80	ENE	c	85	1	0.0	0.4	1.40	0.62	84	0	0.0	0.3	0.96	0.63
	1.22	SSE	v	85	2	0.2	0.4	1.56	0.2	78	4	0.4	0.4	1.27	0.57
	2.27	W	c	63	1	0.9	0.3	1.70	0.85	71	1	2.1	0.6	1.60	0.91
	2.32	WSW	c	63	1	0.9	0.3	1.82	0.76	70	1	2.1	0.6	1.60	0.86
400	0.18	NE	c	85	5	0.0	0.0	2.06	0.55	80	2	0.0	0.0	2.09	0.61
	0.96	S	c	80	1	2.4	0.2	1.90	0.72	74	1	0.0	0.4	2.19	0.68
	1.23	S	v	81	8	2.3	0.2	2.13	0.52	70	1	0.1	0.4	2.11	0.78
	3.10	W	c	50	1	0.9	0.3	1.80	0.85	71	1	0.9	0.5	1.40	0.86
	3.18	W	c	39	7	0.9	0.3	2.60	0.84	67	6	0.9	0.5	2.43	0.68

Table 4. Field experiment conditions for the DP solid-set evaluations arranged in downwind (DP_{dw}) and upwind (DP_{uw}) orientation. Experimental results, calibrated and validated parameters and statistics between measured and simulated water distribution patterns were presented.

Pressure (kPa)	Predom. WS (ms^{-1})	Dir.	Use	DP_{dw}						DP_{uw}					
				CUCe (%)	ΔCUC (%)	K_1	K_2	RMSE	r	CUCe (%)	ΔCUC (%)	K_1	K_2	RMSE	r
200	0.39	SE	c	62	2	4.9	0.04	1.94	0.83	59	1	0.0	0.00	1.59	0.86
	0.52	NNW	c	53	2	4.9	0.04	1.67	0.85	63	2	0.0	0.00	2.14	0.75
	1.02	N	c	52	0	3.1	0.23	1.67	0.88	62	6	0.3	1.37	2.34	0.59
	1.16	NNW	v	59	2	2.5	0.44	2.01	0.8	48	12	1.6	0.12	3.15	0.71
	1.43	ESE	v	60	5	0.7	0.71	2.38	0.65	33	9	2.8	0.21	1.34	0.91
	1.51	SE	c	60	3	0.5	0.75	3.73	0.42	42	2	2.9	0.22	1.89	0.82
	2.06	WNW	c	70	3	3.8	0.69	1.92	0.60	17	5	1.9	0.33	1.35	0.91
	2.40	WNW	c	70	3	3.8	0.69	2.45	0.59	16	5	1.9	0.33	1.85	0.85
	3.25	W	c	66	3	0.3	0.65	1.77	0.81	0	0	0.3	0.68	1.33	0.93
	3.31	W	c	66	3	0.3	0.65	2.37	0.66	0	0	0.3	0.68	1.29	0.96
300	0.35	SE	c	53	3	4.6	0.01	2.39	0.87	64	4	0.0	0.00	1.52	0.90
	0.35	S	c	54	0	4.6	0.01	2.17	0.91	61	2	0.0	0.00	1.62	0.88
	0.80	ENE	c	51	7	1.7	0.02	2.37	0.85	56	5	1.7	0.02	2.85	0.75
	1.22	SSE	v	54	4	1.5	0.07	4.38	0.37	48	5	1.9	0.04	1.62	0.92
	1.45	SE	v	49	9	1.2	0.13	2.84	0.69	65	6	2.1	0.05	1.55	0.92
	1.66	N	c	45	3	2.1	0.12	1.83	0.92	64	5	0.7	1.32	2.72	0.61
	2.27	W	c	68	0	0.3	0.31	2.53	0.75	1	8	2.7	0.11	1.36	0.95
	2.32	WSW	c	65	3	0.3	0.31	3.40	0.63	7	6	2.7	0.11	1.46	0.94
	2.67	WSW	c	66	7	4.0	1.82	1.57	0.88	3	7	2.8	0.01	1.85	0.89
	3.04	WSW	c	62	8	4.0	1.82	2.02	0.84	0	3	2.8	0.01	1.34	0.94
400	0.18	NE	c	62	3	3.7	0.05	1.39	0.96	67	2	0.0	0.00	1.92	0.82
	0.36	NNE	c	56	2	3.7	0.05	1.61	0.94	61	2	0.0	0.00	1.68	0.87
	0.96	S	c	56	5	0.3	0.04	4.03	0.69	58	0	2.4	0.11	2.17	0.85
	1.23	S	v	58	8	3.3	0.30	3.59	0.57	55	5	0.4	0.13	2.54	0.81
	1.35	WSW	v	62	5	3.1	0.38	2.86	0.65	36	25	0.5	0.17	2.74	0.86
	1.59	SSE	c	57	7	3.1	0.39	4.03	0.62	55	1	0.5	0.18	2.53	0.83
	2.30	W	c	65	2	0.2	0.38	2.57	0.77	24	1	2.4	0.24	2.10	0.90
	2.98	WNW	c	64	9	0.0	0.30	2.36	0.76	0	0	0.9	0.23	1.82	0.93
	3.10	W	c	66	1	0.2	0.38	2.77	0.77	0	0	0.9	0.23	1.24	0.96
	3.18	W	c	63	4	0.0	0.30	3.05	0.81	0	0	0.9	0.23	1.24	0.96

Table 5. Simulated irrigation dose (ID, mm), Irrigated collected (IDc, mm), average CUC (%), seasonal CUC (%) and corn yield (%) for the sprinkler irrigated areas for each sprinkler type and orientation and for the total plot area equipped with PC(1Noz), or PC(2Noz) or DP sprinklers as plot-boundaries irrigation solutions.

	Sprinkler type	ID (mm)	IDc (mm)	$CUC_{ave.}$ (%)	$CUC_{seas.}$ (%)	Yield (%)
Sprinkler irrigated area	FC	641.0	588.4	85.5	90.0	95.0
	PC_{dw}(1Noz)	651.9	551.7	76.8	92.5	96.8
	PC_{uw}(1Noz)	651.9	591.1	83.1	90.4	93.5
	PC_{dw}(2Noz)	799.5	687.9	77.4	90.2	99.6
	PC_{uw}(2Noz)	799.5	690.1	71.5	82.1	95.6
	DP_{uw}	975.4	699.9	61.9	68.2	99.7
	DP_{dw}	975.4	840.5	54.5	71.8	97.0
Total Plot area	PC (1Noz)	**652.0**	582.9	83.7	**90.5**	**95.0**
	PC(2Noz)	**700.4**	621.4	81.9	**88.7**	**95.9**
	DP	**684.7**	617.3	83.5	**88.9**	**95.3**

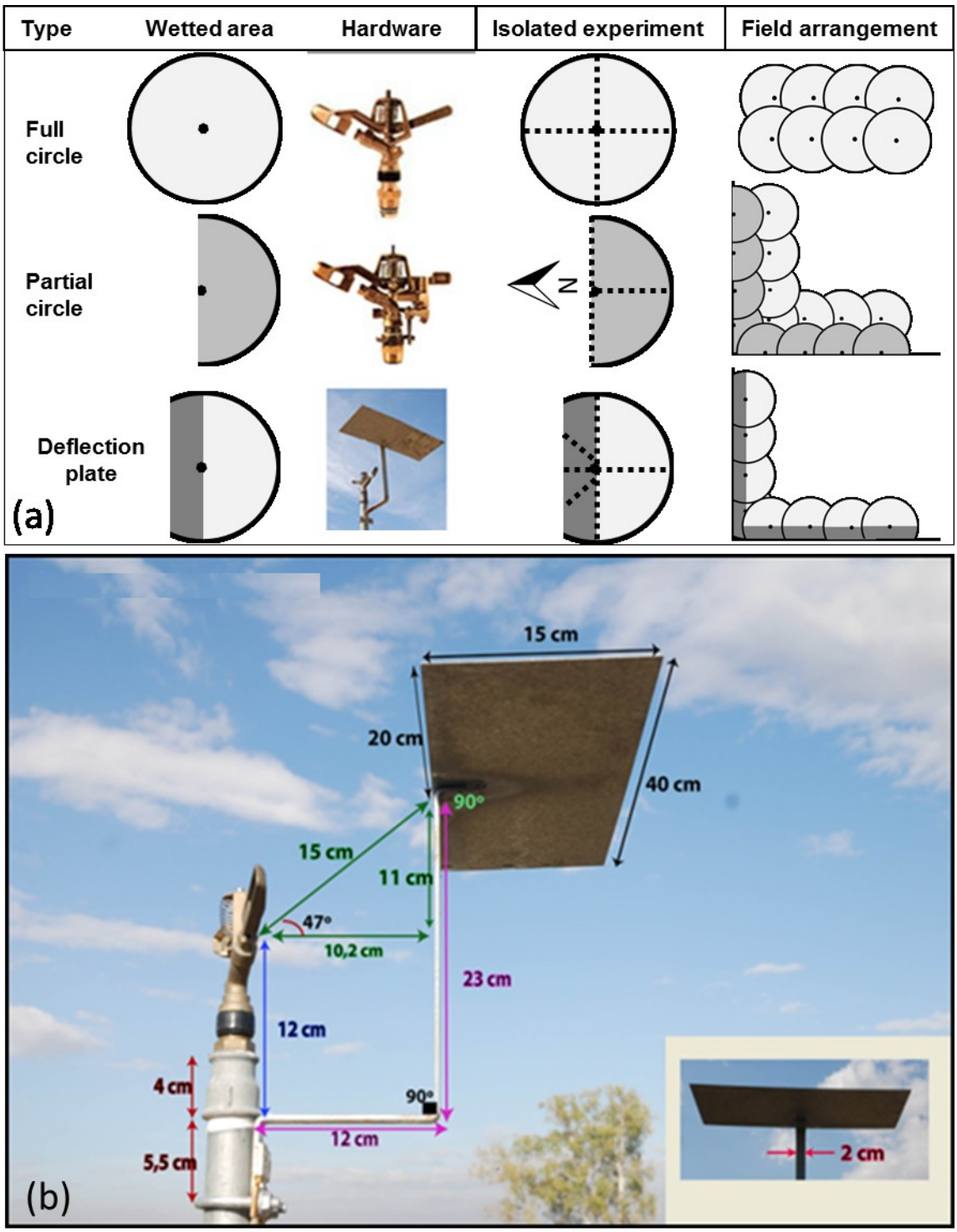

Figure 1. Evaluated Field boundaries sprinklers with its field arrangement (a) and the shape of the deflecting plate (b).

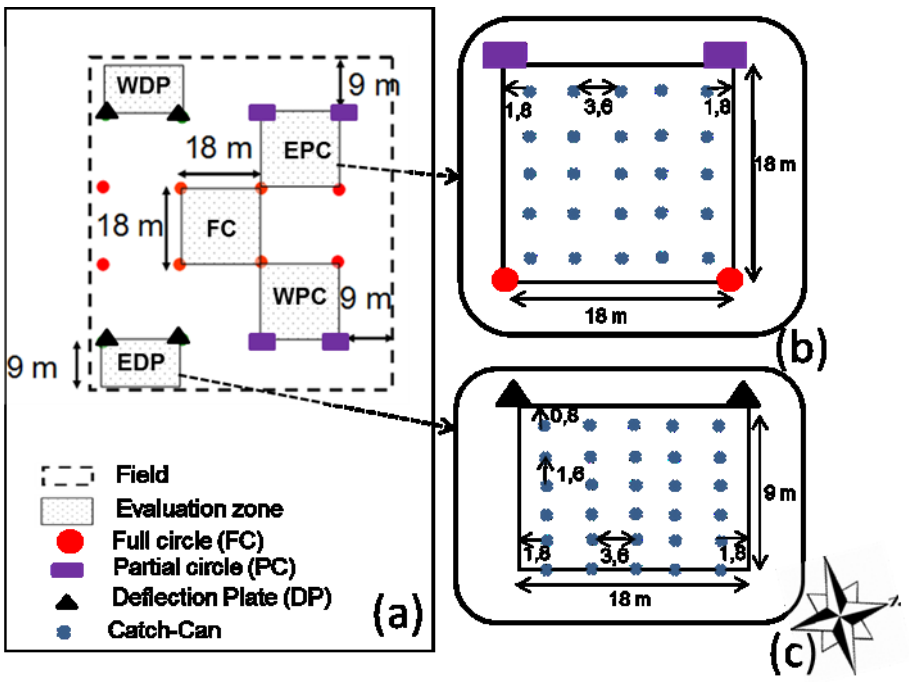

Figure 2. Solid-set experimental plot design. Evaluation area and catch-can configurations for FC, PC and DP sprinklers were detailed. For PC and DP sprinklers two orientations were considered for evaluation, west (WPC and WDP) and east (EPC and EDP).

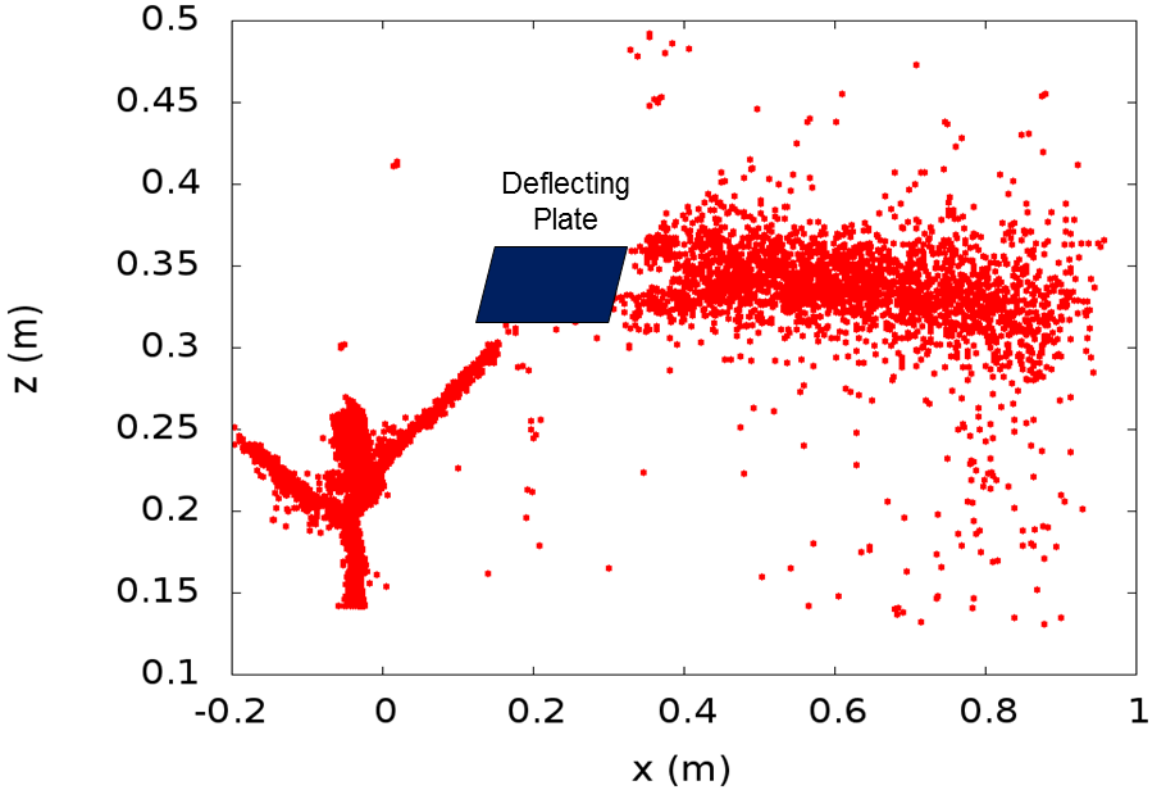

Figure 3. Morphology of the sprinkler jet after the impact with the deflecting plate and location of the drops in their trajectory after the plate impact obtained with the 3D scanner.

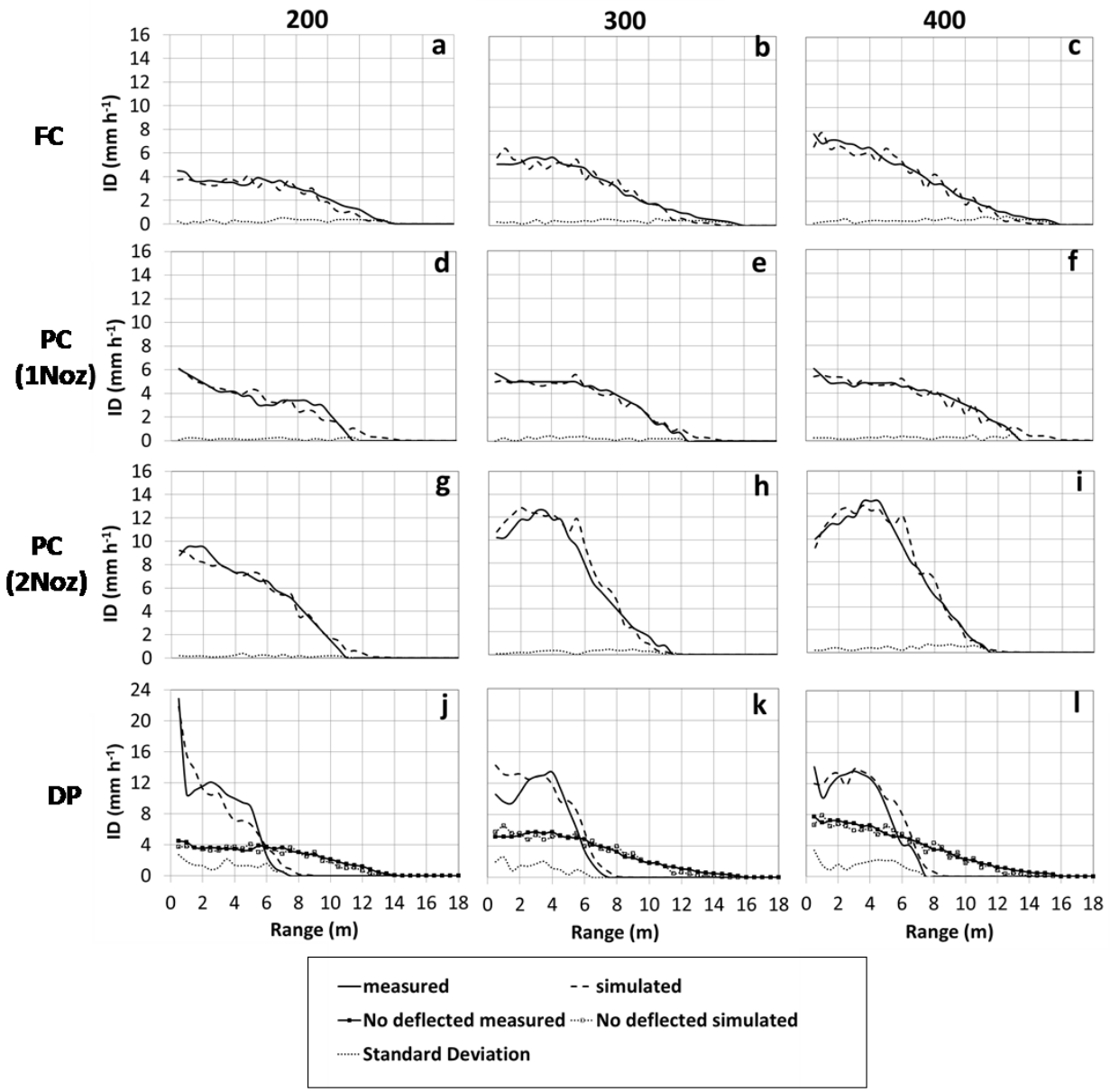

Figure 4. Measured (solid lines) and simulated (dashed lines) radial water application pattern for the experimental FC, PC (1Noz), PC (2Noz) and DP sprinklers operating at 200, 300 and 400 kPa.

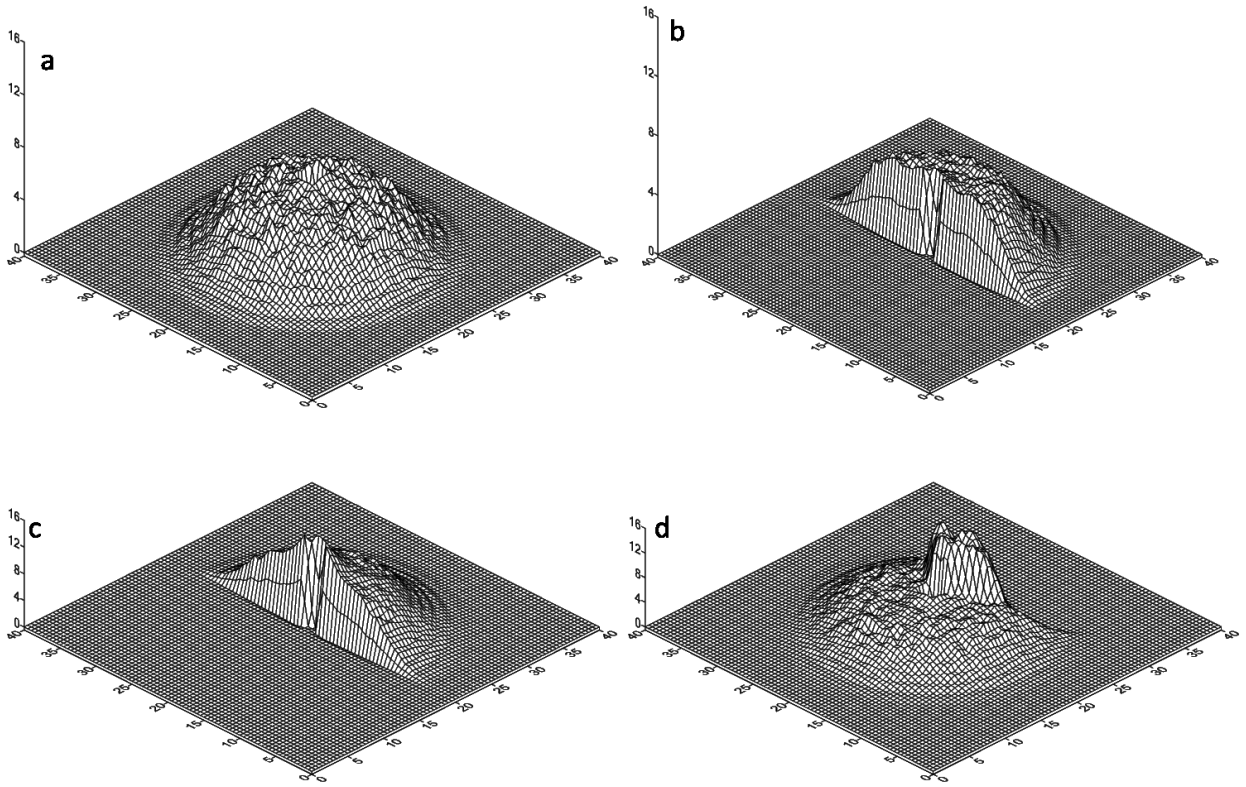

Figure 5. 3-dimensional simulation of water distribution pattern for isolated FC (a); PC (1Noz) (b); PC (2Noz) (c) and DP sprinklers (d) operating at 300 kPa.

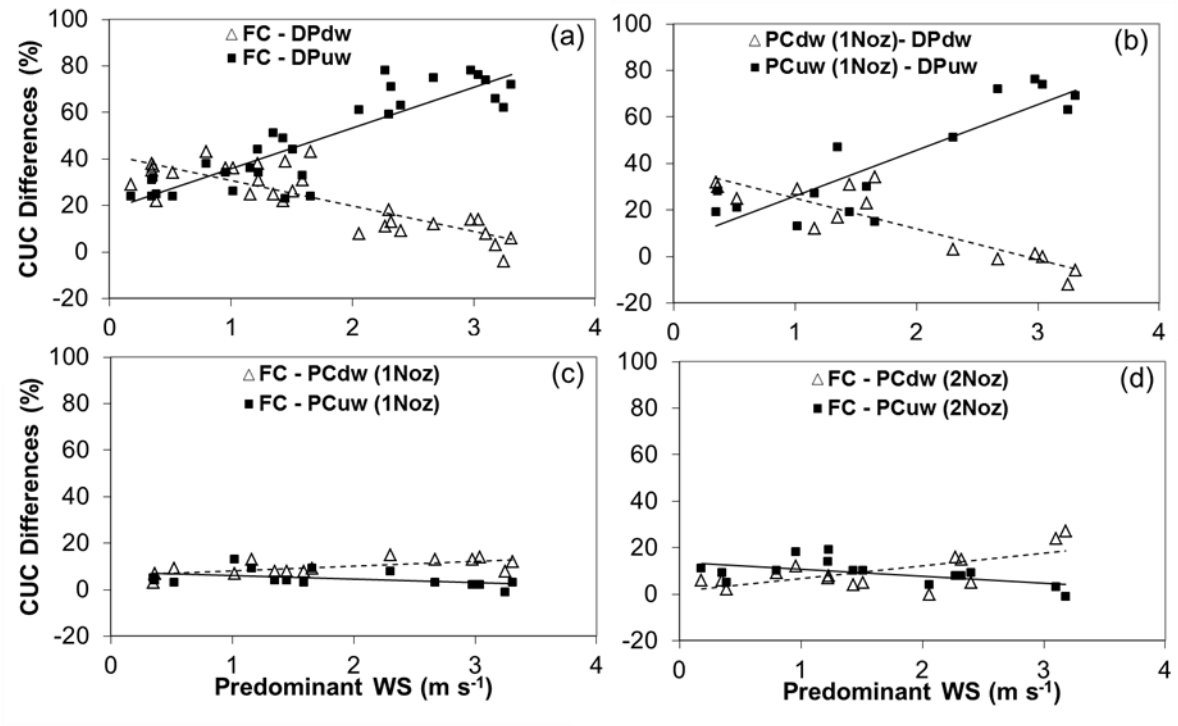

Figure 6. Evolution of the CUC differences (%) as a function of wind speed between FC and DP areas (a); between PC (1Noz) and DP areas (b); between FC and PC (1Noz) areas (c); and between FC and PC (2Noz) areas (d) for the two evaluated orientations.

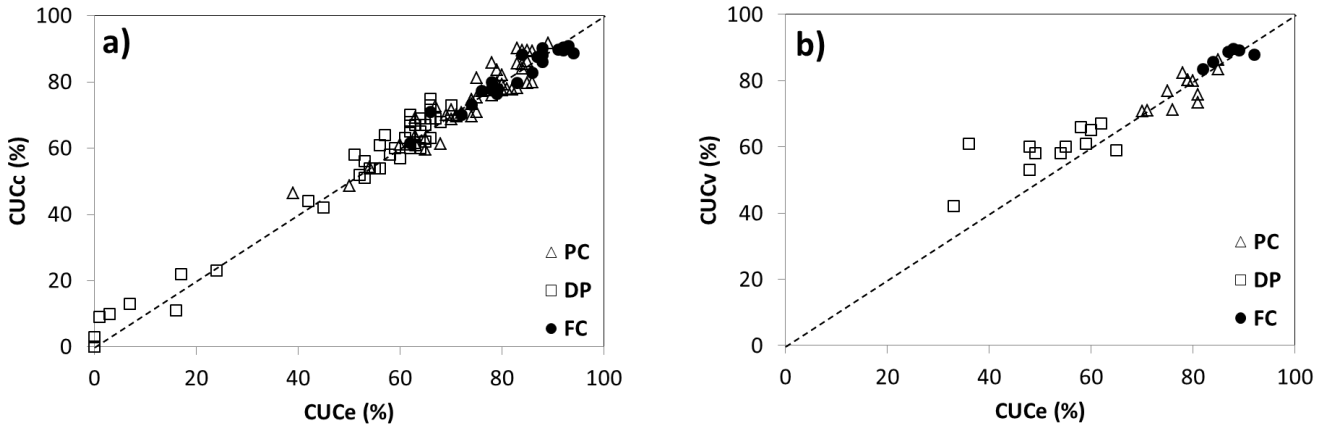

Figure 7. Experimental vs. calibration coefficients of uniformity (CUC_e and CUC_c, respectively) (a) and experimental vs. validation coefficients of uniformity (CUC_e and CUC_v, respectively) (b) for FC, PC and DP sprinklers. The dashed line represents the 1:1 relationship.

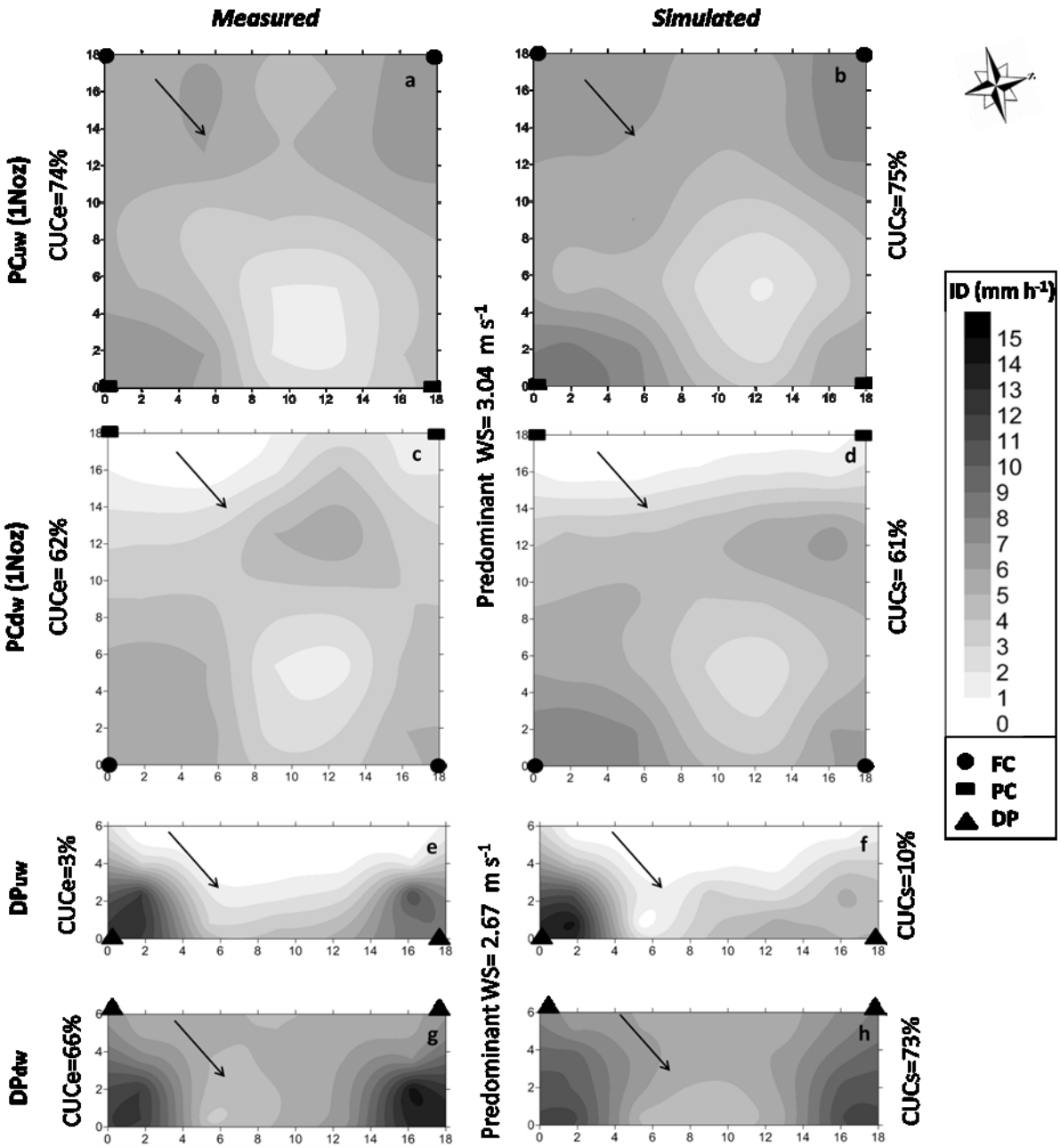

Figure 8. Contour maps of the water distribution pattern (ID, mm h^{-1}) for the experimental (left) and simulated (right) PC(1noz) and DP sprinklers at a working pressure of 300 kPa under moderate wind speed. Upwind and downwind jet orientations were presented. Arrows indicate the prevailing wind direction during each event. Wind speed (WS) and Christiansen uniformity coefficient measured (CUC_e) and simulated (CUC_s) are indicated in the figures.

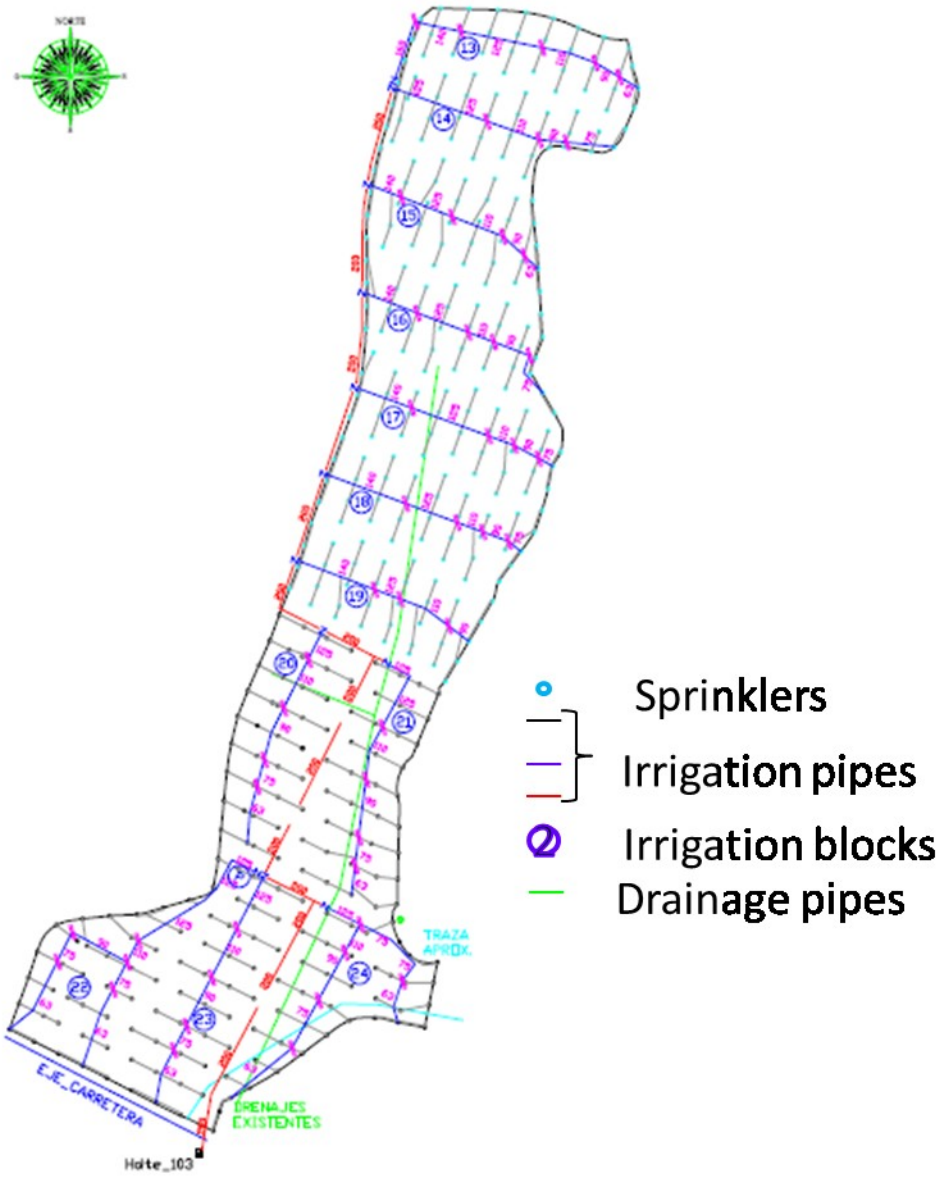

Figure 9. Commercial plot designed with PC as sprinkler plot-boundaries solutions (designs 1 and 2).